PEAT

PROGRESS IN ENGINEERING APPLICATION AND TECHNOLOGY
e-ISSN: 2773-5303

Vol. 7 No. 2 (2026) 196-202
https://publisher.uthm.edu.my/periodicals/index.php/peat

Structural Analysis and Design Improvement of the Lightweight Applicator Handheld Spreader Frame Using Solidworks Simulation

Noor Iman Zidane bin Loo Su Pin[1], Khairu Kamaruddin[1]*, Mohd Nazri Hasim[2]

[1] *Department of Mechanical Engineering Technology, Faculty of Engineering Technology, Universiti Tun Hussein Onn Malaysia*

[2] *Pejabat Felda Raja Alias 4 Federal Land Development Authority (FELDA), Bandar Baru Serting, 72120 Bandar Seri Jempol, Negeri Sembilan, MALAYSIA*

*Corresponding Author: khairu@uthm.edu.my
DOI: https://doi.org/10.30880/peat.2026.07.02.024

Article Info

Received: 26 June 2026
Accepted: 11 August 2026
Available online: 10 November 2026

Keywords

Lightweight Applicator Handheld Spreader, Design for Manufacturability, Computer Aided Design, Finite Element Analysis, Factor of Safety, AISI 304

Abstract

Manual fertilizer application in oil palm plantations presents significant ergonomic hazards due to the excessive weight of conventional equipment. This research addresses these challenges by structurally analyzing and optimizing the geometric parameters of the Lightweight Applicator Handheld Spreader (LAHS) frame. A virtual prototyping methodology was employed using SolidWorks Simulation. The model utilized 2-D Shell Elements with localized mesh controls applied to welded connections to accurately capture singular stress gradients under a 47.2 kg operational load. Initial baseline simulations revealed significant over-engineering of the prototype, prompting a three-stage parametric optimization process guided by strict Design for Manufacturability (DFM) constraints. The final optimized geometry achieved a 36.09% mass reduction, utilizing commercially available AISI 304 stainless steel (19.1 mm square tubing and 25.4 mm circular handles). Computational validation confirmed the structure maintained a minimum Factor of Safety (FOS) of 2.092 and a maximum structural deflection of 2.851 mm, ensuring both operational safety and improved maneuverability.

1. Introduction

As an emerging subject of strategic management in high value production of oil palm plantation, proper nutrient management is crucial to maximize yield efficiency (İrsel Gürkan, 2021). But the hard ground of these areas sometimes makes it impractical to use large machines (Berardi et al., 2025), and it results in large-scale use of manual methods which leads to exhaustion (Meng X, 2024). In this context, the "strength-to-weight ratio" is the major factor distinguishing manual agricultural tools; the equipment has to be robust enough to endure the rigors of farm life, but still light enough so as to be easy for an operator to work (Berardi et al., 2025; Hainan & Yang, 2025).

A main engineering challenge in the design of the Lightweight Applicator Handheld Spreader (LAHS) is maintaining the required strength while simultaneously avoiding the risk of Hand-Arm Vibration Syndrome (HAVS) and Musculoskeletal Disorders (MSDs). High force/weight to grip and physical exertion with the added

This is an open access article under the CC BY-NC-SA 4.0 license.

vibration transmission creates long-term health risks (Peng Yin et al., 2019; Widia & Dawal, 2011). The original LAHS prototype showed that it was non-optimally designed and due to this it did not have a structural evaluation for the maximum operational load it faced, which was defined as 47.2kg (Lim et al., 2023). This load consisted of a 45kg payload and a 2.2kg offset battery making an unnecessary load on the frame, which has its main ergonomic advantage (İrsel Gürkan, 2021).

The main aim of this research is to find an optimized frame design, which gives the right balance between structural strength and ergonomic weight reduction. This study seeks to optimize the maneuverability of the spreader and safety of the workers by identification and removal of the "lazy material" from the low stress area. To meet these challenges, a robust computational approach must be used to guarantee that weight reduction does not adversely affect the reliability of the tool in use in field conditions.

2. Methodology

A non-destructive testing method that was used was Finite Element Analysis (FEA) as a way of modifying designs as quickly as possible without the costly expense of physical prototyping. The mapping of stress concentration can be achieved virtually and the geometric parameters can be systematically modified.

2.1 Materials

The frame has been designed using AISI 304 Stainless Steel to provide high strength in a low weight material and can resist corrosion. The mechanical properties used for the simulation are listed in the Table 1.

Table 1 *Mechanical Properties of Stainless Steel (AISI 304)*

Property	Symbol	Value	Unit
Yield Strength	σ	206.8	MPa
Elastic Modulus	E	190	GPa
Mass Density	ρ	8000	kg/m^3
Poisson's Ratio	v	0.29	N/A

2.2 FEA Setup

Shell Mesh Elements were used to discretize the geometry. This approach was selected over beam elements to accurately capture localized stress gradients at welded junctions. To ensure computational reliability and eliminate artificial stress singularities, localized mesh controls were applied at critical transitions. Furthermore, a mesh independence study was conducted on the baseline geometry to verify numerical convergence. Global element sizes were iteratively reduced from 20 mm to 5 mm while monitoring the maximum Von Mises stress at the critical rear axle joint. Convergence was achieved when the stress variance between successive refinements fell below 5%, establishing the optimal mesh density for all subsequent parametric studies. The LAHS was modeled as a Class 1 Lever system, with the rear axle functioning as an immovable fulcrum and the handlebar set as the effort point (Reference Geometry). These constraints allowed free longitudinal (Z-axis) translation, enabling realistic bending simulations of the main structural spine.

2.3 Loading Conditions

The simulation applied static loads representing a worst-case operational scenario of 47.2 kg total mass:

- **Vertical Force (Hopper/Motor):** 441.45 N (representing a 45 kg mass) applied at the primary mounting pivots.
- **Offset Force (Battery):** 21.582 N (representing a 2.2 kg mass) applied asymmetrically to the right side of the chassis mid-span.

2.4 Optimization Strategy

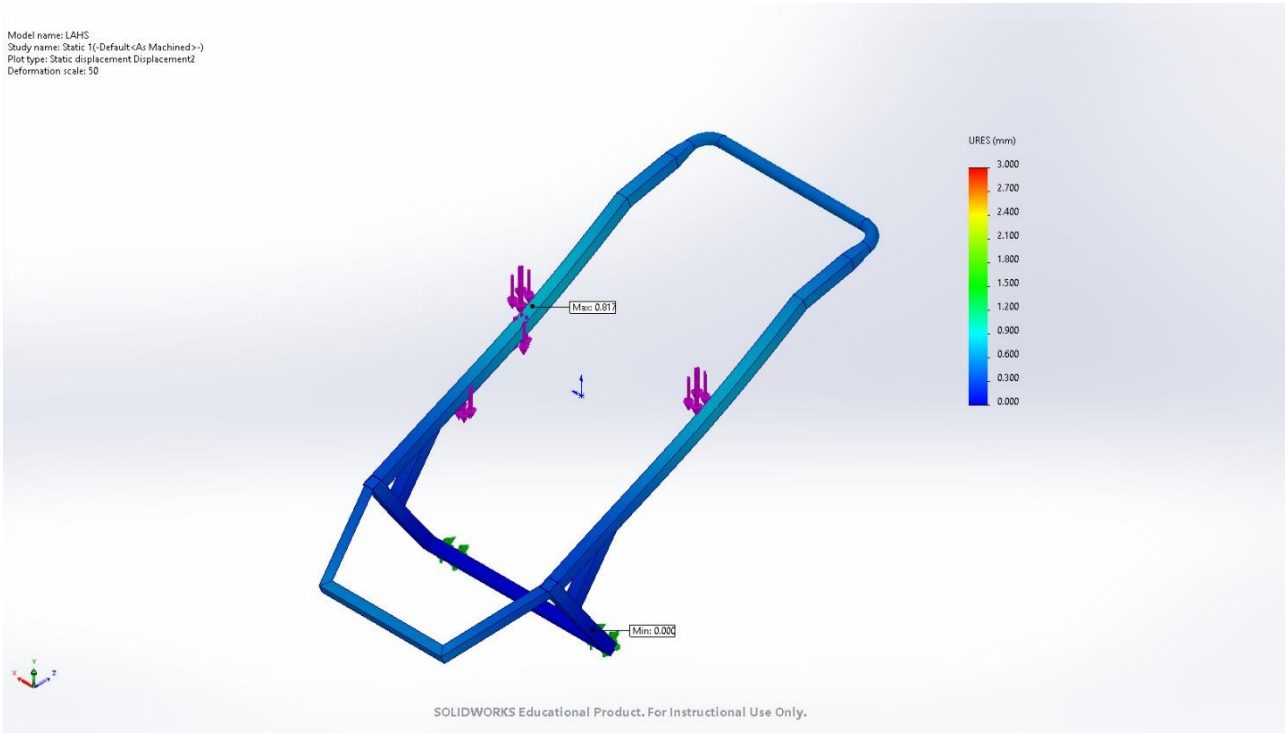
This study applied Parametric Size Optimization for optimization of the size (thickness and diameter) of standard tubular profile. There were two critical safety guidelines to follow: 1) the Factor of Safety was less than 2.0 and 2) the Maximum Structural Deflection was less than 3.0 mm. The foundation for optimizing in the following 3 stages was these controlled variables in order to maximize material efficiency.

3. Result and Discussion

The results reveal the basic "Mass-Stiffness Trade-off". When the material is being trimmed to achieve weight reduction, then the structure's natural compliance naturally increases and the code must be validated to ensure that the increased flexibility will not exceed safe operating conditions.

3.1 Baseline Performance

The original frame was evaluated to find an FOS of 3.87. Dark blue stress contour areas were the predominant ones in chair plane stress contour plots, representing "lazy material" with stresses of less than 10 MPa. This meant that the building was heavily weighted but with it reducing vital loads, it had been identified that mass could be removed.

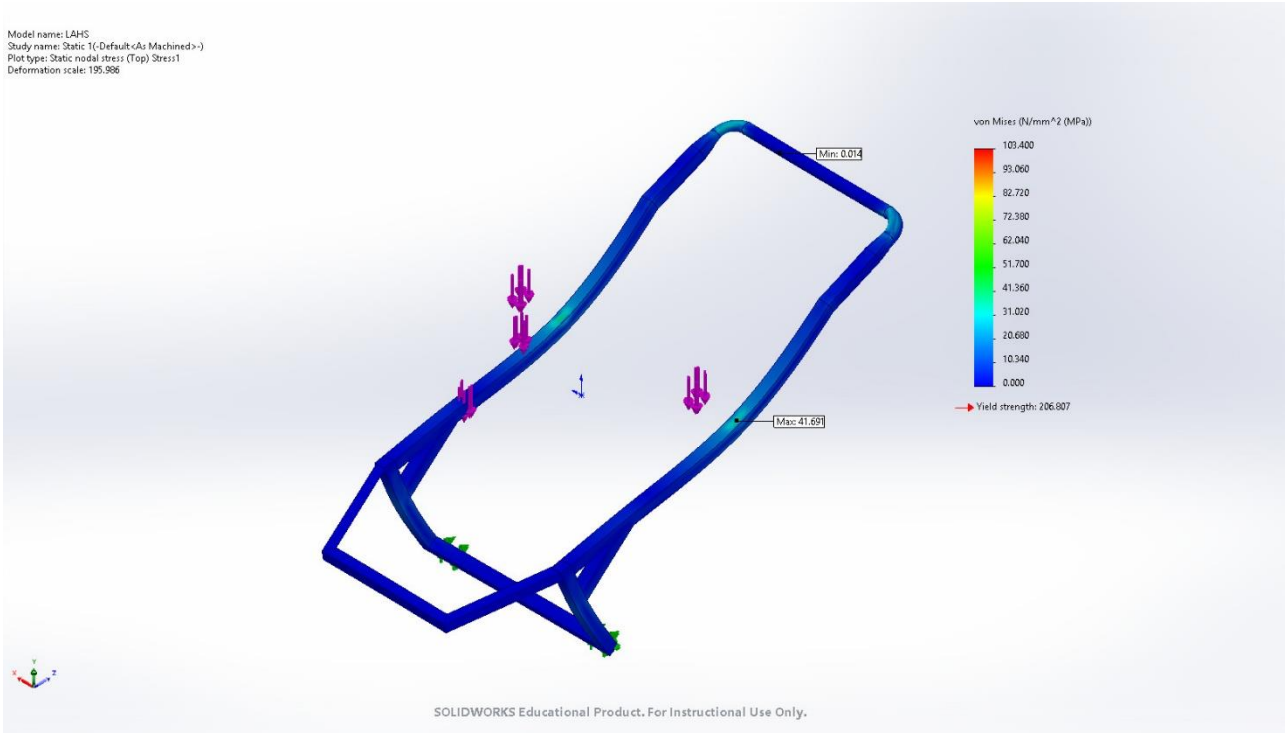


(a)



(b)

Progress in Engineering Application and Technology Vol. 7 No. 2 (2026) p. 196-202



(c)

Figure 1 *(a) Baseline Simulation Displacement Results (b) Baseline Simulation Factor of Safety Results (c) Baseline Simulation Stress Results*

3.2 Optimization Iterations

Table 2 summarizes the transition from the over-engineered baseline to the final optimized design.

Table 2 *Frame Dimensions and Performance Comparison*

Metric	Baseline	Iteration 1	Iteration 2	Iteration 3 (Final)
Tube Profile (Chassis)	30.0 mm	22.0 mm	22.0 mm	**19.1 mm**
Tube Profile (Handle)	30.0 mm	22.2 mm	22.0 mm	**25.4 mm**
Wall Thickness	1.2 mm	0.8 mm	0.8 mm	**1.0 mm**
Frame Mass	5,424.21 g	3,364.77 g	3,305.34 g	**3,466.72 g**
Min FOS	3.87	2.25	2.23	**2.092**
Max Deflection	0.817 mm	2.439 mm	2.525 mm	**2.851 mm**

(1)

As observed in Table 2, the transition from the baseline model to the finalized Iteration 3 demonstrates the fundamental mass-stiffness trade-off inherent in structural mechanics. To achieve the 36.09% mass reduction (from 5,424.21 g to 3,466.72 g), the geometric profile of the main square chassis was shrunk from 30.0 mm to 19.1 mm. By reducing the outer dimensional footprint, the Area Moment of Inertia of the structural members was significantly reduced. Consequently, the structure's global elasticity naturally increased, which is reflected in the maximum deflection rising from a rigid 0.817 mm in the baseline to 2.851 mm in the final design. Similarly, the localized von Mises stress increased, driving the global Factor of Safety (FOS) down from 3.87 to 2.092. However, this controlled flexibility represents a highly successful engineering compromise. By establishing strict safety constraints prior to the parametric study, the solver ensured that the increased deflection remained well below the 3.0 mm operational limit and the FOS remained safely above the 2.0 threshold, confirming that absolute rigidity is unnecessary and physically detrimental to the tool's ergonomic goals.

3.3 The DFM Pivot (Iteration 3)

Iteration 2 was the mathematically ideal solution but was turned down, however it had demonstrated a “Design for Manufacturability” (DFM) change. The 0.8 mm wall thickness requested in Iteration 2 was very susceptible to

'burn through' during TIG welding. Therefore, for Iteration 3, standard wall thickness outside diameter (1.0 mm) was used. To obtain the desired wall thickness and target weight, the square tube profile was thinned to 19.1 mm and the handles were set at 25.4 mm circular tubular to ensure that the user was not harmed. The balance in this method, created to keep the frame both light and easy to build, resulted in a significant increase in the number of fabrication facilities being able to produce the frame.

3.4 Impact on SDGs

The completed design attributes of 3.47kg corresponds with 4 of the UN Sustainable Development Goals:

- **SDG 3 (Good Health and Wellbeing):** By improving REBA (Rapid Entire Body Assessment) postures, decreasing the grip force needed, and directly reducing the weight being lifted, the 36.09% weight reduction directly contributes to improving the 'Physical Risk Score' risk reduction component.
- **SDG 9 (Industry, Innovation, and Infrastructure):** Shows use of advanced FEA to improve the design of agricultural tools in the region.
- **SDG 12 (Responsible Consumption and Production):** Raw materials are also significantly reduced by using in such a way that it promotes resource efficiency. The final design fits neatly into the field and is balanced for both easier movement and good high performance engineering design.

4. Conclusion

The 36.09% mass reduction resulted from a three-stage parametric study by performing FEA and were successfully validated in this research that led to the primary objective of optimizing the LAHS frame for ergonomic safety. The key messages are:

- **Material Efficiency:** Removed 1,957.49 g of excess material identifying this material would have been more efficient and in turn the tool would have been more maneuverable.
- **Structural Integrity:** The thinned frame has been tested with peak asymmetric loading to verify the frame can have a FOS of 2.092 for plantation durability.
- **Manufacturing readiness**: Drawing upon experience accumulated at processing 1.0 mm, standard stock and 25.4 mm handles, the manufacturing readiness of a DFM-compliant model for immediate local manufacturing is the goal. Selected for future work will be the physical prototyping and field deployment of the optimized frame, to provide confirmation of the expected durability over time of the frame under dynamic loading conditions.

Acknowledgement

The authors would like to express their gratitude to the Faculty of Engineering Technology, Universiti Tun Hussein Onn Malaysia (UTHM) for supporting this research. Special appreciation is extended to the Federal Land Development Authority (FELDA) for providing access to the machinery required for technical measurements and field data collection.

Conflict of Interest

Authors declare that there is no conflict of interests regarding the publication of the paper.

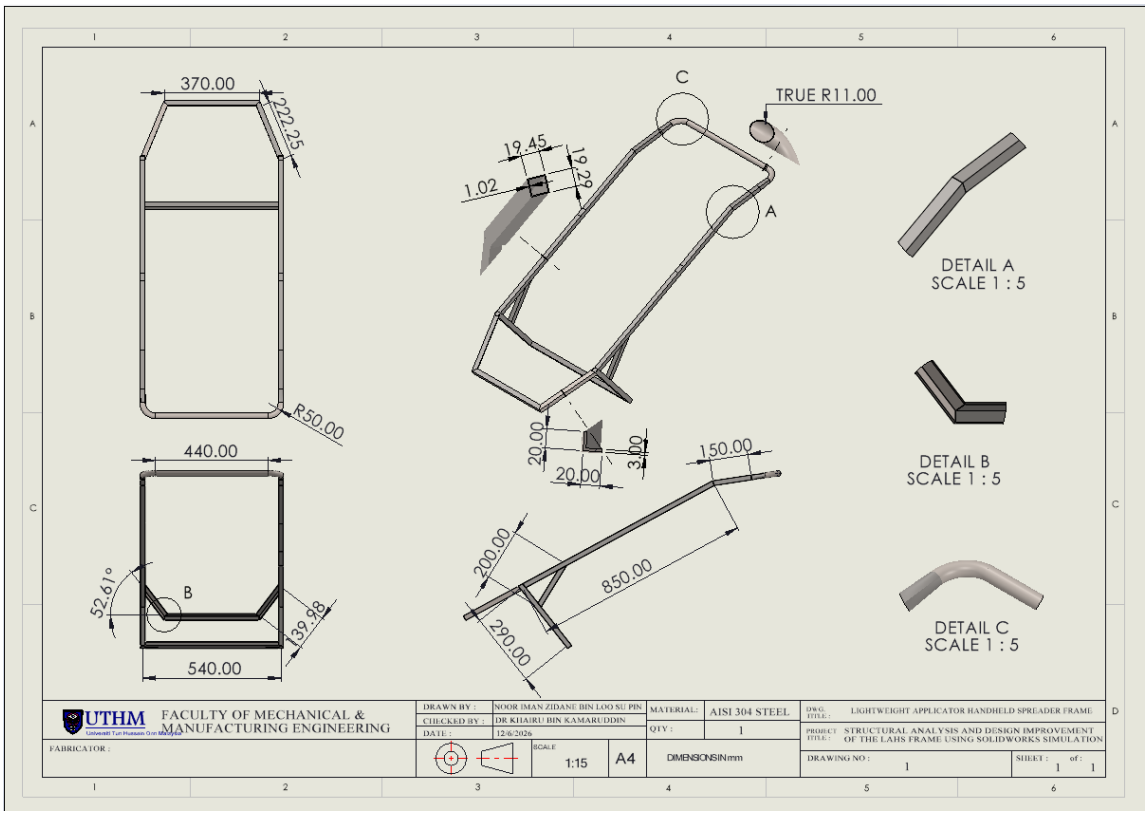
Author Contribution

This journal requires that all authors take public responsibility for the content of the work submitted for review. The contributions of all authors must be described in the following manner:

The authors confirm contribution to the paper as follows: ***study conception and design:*** *Khairu, Noor;* ***data collection:*** *Noor, Nazri;* ***analysis and interpretation of results:*** *Noor, Nazri;* ***draft manuscript preparation:*** *Noor. All authors reviewed the results and approved the final version of the manuscript.*

Appendix A: SolidWorks Drawing

Progress in Engineering Application and Technology Vol. 7 No. 2 (2026) p. 196-202



References

Journal

Ashraf, M., Gardner, L., & Nethercot, D. A. (2008). Structural stainless steel design: Resistance based on deformation capacity. *Journal of Structural Engineering*.

Berardi, A., dellisanti, C., Tarantino, D., Ouette, K., Leone, A., & Tamborrino, A. (2025). FEA for optimizing design and fabrication of frame structure of elevating work platforms. *Applied Sciences*, *15*(13), Article 7356. https://doi.org/10.3390/app15137356

Dissanayake, L. N., Walport, F., Yun, X., & Gardner, L. (2025). Unified stress-strain models for normal and high strength steels. *Construction and Building Materials*, *459*. https://doi.org/10.1016/j.conbuildmat.2024.139616

Haupt, W., Borges, L., Israel, C., & Riffel, K. (2024). Effects of laser welding on the mechanical properties and microstructure of AISI 304 stainless steel. *Lasers in Manufacturing and Materials Processing*. https://doi.org/10.1007/s40516-024-00268-3

Irsel, G. (2021). Strength-based design of a fertilizer spreader chassis using computer aided engineering and experimental validation. *Proceedings of the Institution of Mechanical Engineers, Part C: Journal of Mechanical Engineering Science*, *235*, 095440622199384. https://doi.org/10.1177/0954406221993847

Irsel, G. (2023). Design of a precision planter chassis using computer-aided engineering and experimental validation. *Proceedings of the Institution of Mechanical Engineers, Part C: Journal of Mechanical Engineering Science*, *237*, 5426-5442. https://doi.org/10.1177/09544062231159008

Li, H., & Li, Y. (2025). Finite element analysis and structural optimization design of multifunctional robotic arm for garbage truck. *Frontiers in Mechanical Engineering*, *11*. https://doi.org/10.3389/fmech.2025.1543967

Liang, C. (2022). Application and prospect of analysis of structures based on finite element method. *Highlights in Science, Engineering and Technology*, *28*. https://doi.org/10.54097/hset.v28i.4059

Lim, R. G., Kim, W.-S., Do, Y.-W., Siddique, M., & Kim, Y.-J. (2023). Performance evaluation of a virtual test model of the frame-type ROPS for agricultural tractors using FEA. *Agriculture*, *13*(10), Article 2004. https://doi.org/10.3390/agriculture13102004

Meng, X. (2024). Weight reduction strategies in chassis design without compromising safety. *Advances in Automobile Engineering*, *13*, Article 289.

Saygili, Y. S., & Çakmak, B. (2025). Use of finite element method in agricultural machinery and application examples. *Ege Üniversitesi Ziraat Fakültesi Dergisi*, *62*(3), 407-419. https://doi.org/10.20289/zfdergi.1638358

Tawk, C., & Alici, G. (2020). Finite element modeling in the design process of 3D printed pneumatic soft actuators and sensors. *Robotics*, *9*(3), Article 52. https://doi.org/10.3390/robotics9030052

Tovt, B., Leontiev, D., & Malyi, V. (2025). Formulation of the problem of topology optimization of automobile and agricultural machinery structures. *Автомобільний транспорт (Automobile Transport)*, *56*. https://doi.org/10.30977/AT.2219-8342.2025.56.0.03

Tyflopoulos, E., & Steinert, M. (2020). Topology and parametric optimization-based design processes for lightweight structures. *Applied Sciences*, *10*(13), Article 4496. https://doi.org/10.3390/app10134496

Vemula, A., Kamal, O., Rithik, K., & Tarun, K. (2025). Design optimization and structural analysis of SAE BAJA chassis using Solidworks and Ansys. *International Journal on Science and Technology*, *16*(2). https://doi.org/10.71097/ijsat.v16.i2.6223

Widia, M., & Dawal, S. (2011). The effect of hand-held vibrating tools on muscle activity and grip strength. *Australian Journal of Basic and Applied Sciences*, *5*(11), 198-211.

Yin, P., Yang, L., Wang, C., & Qu, S. (2019). Effects of wearable power assist device on low back fatigue during repetitive lifting tasks. *Clinical Biomechanics*, *70*, 59-65. https://www.sciencedirect.com/science/article/pii/S0268003318308143

Zhou, S., Chen, Q., & Zhang, L. (2025). Sensitivity analysis based on E-TOPSIS combined with MORIME-based multi-objective optimization for sprayer frame design optimization. *Machines*, *13*(3), Article 201. https://doi.org/10.3390/machines13030201